Chemical Synthesis of Marble Powder-Fly Ash Doped Poly (Vinyl Alcohol) Composites and Comparison between their Structural, Thermal and Mechanical Properties

Canan A. Canbay* and N. Ünlü

Department of Physics, Faculty of Science, Firat University, Elazig, Turkey

Abstract: In this study, poly (vinyl alcohol) based composite materials were produced. Fly ash and Karaman Beige and Rosso Levanto marble powders were taken by Alacakaya Marble and Mining Business and they were used as fillers. Composite materials (at the rate of 1/20 by mass) were produced. The microstructure analysis of the materials was examined by Scanning Electron Microscope. Fourier Transform Infrared Spectrophotometer analysis was used to get information about the functional groups in the structures of the materials. The thermal behavior of the materials was analyzed by Differential Thermal Analysis and Differential Scanning Calorimetry at the same single heating rate of 10 C/min. X-Ray Diffraction analysis was performed to determine the crystallographic properties of the materials at room temperature. The mechanical and physical properties of the obtained materials were examined by stress-strain analysis.

Keywords: Poly (vinyl alcohol), Composite materials, Marble powder, Fly ash content, Characterization results.

1. INTRODUCTION

Limestones ($CaCO_3$) and dolomitic limestones ($CaMg(CO_3)_2$) are minerals that have undergone metamorphism and can be recrystallized [1]. These stones, which have gained new structures, are called marble. This general metamorphism is formed by vigorous pressure at very deep and the effect of temperature. Marble, which is generally used as a decorative building material turns into powder during operations such as cutting, shaping, and polishing, approximately 25% of its mass. Turkey has 40% (about $5.2x10^9$ m^3) of the total marble reserves in the world. In our country where 7.000.000 tons of marble is produced annually, there are significant losses in both the extraction and processing of marbles. 75% of the produced marble is processed in 5000 processing plants. Therefore, it becomes difficult to stock millions of tons of waste material accumulated in these plants [2,3]. Fly ash is an industrial waste obtained as a result of flue gas filtration in thermal power plants [4]. There are light metal oxides in the basic structure of fly ash, whose particles are spherical. Fly ash is a material that is widely used in composite materials, thanks to its lightness, micro-grain size, amorphous structure, and cheapness [5]. It is very beneficial to create a usage area for fly ash, which contains a lot of active silica and alumina [6]. Fly ash, which is in waste condition, causes both economic losses and environmental problems like waste marble dust. The evaluation of marble powders and fly ash is very important because it contributes to the economy and reduces environmental pollutants.

*Address correspondence to this author at the Department of Physics, Faculty of Science, Firat University, Elazig, Turkey; Tel: +90(0536)-5256357; E-mail: caksu@firat.edu.tr

Marble powders that can not be used have negative effects not only economically but also environmentally. It is possible to use marble powders stored as waste in different branches of industry for different purposes [7]. In recent years, some studies increase these applications. Terzi *et al*. investigated the use of marble dust wastes as an alternative to aggregate dust in asphalt concrete as filling material. In their study, they showed that marble powders can be used instead of aggregate dust, especially in regions where marble dust is high and transportation/drying cost does not exceed stone dust filler cost [8]. Hirostova *et al*. produced a polyester matrix composite material for the use of marble powders as fillers. Then they examined the effects of marble filling material on physical aging. Therefore, they have achieved their goals by proving the model they have developed theoretically with experimental results [9]. Khristova *et al*. examined the formation properties of a composite material consisting of epoxy resin and marble powders. As a result of this study, they found that the material deforms in the interaction regions of epoxy resin and marble powders [10]. Garcia *et al*. conducted chemical analyzes of marble wastes. They found particles containing 99% carbonate in their structures. They then hypothesized that marble wastes could be used to obtain ceramic products. For this purpose, they showed that it would be appropriate to add marble powder into calcite and dolomite to produce ceramic materials used in wall coverings [11]. Ali *et al*. showed that marble powders can be used to eliminate the instability of traditionally used plaster materials such as lime and cement against some chemical and physical changes. In their study, it was determined that plasters made with a

E-ISSN: 2410-4701/20

mixture of marble powder and hydraulic compounds are resistant to different weather conditions [12]. Ohama has conducted a compilation of recent studies on concrete-polymer composite materials [13].

In this study, composite materials with poly (vinyl alcohol) matrix have been produced. Fly ash that has been taken from Firat University Faculty of Technology, Karaman Beige, and Rosso Levanto marble powders that have been taken from Alacakaya Marble and Minning Business, have mixed with poly (vinyl alcohol) in the same ratio. The produced Karaman Beige marble powder/PVA composite is coded as CM1, Fly ash/PVA composite is named CM2 and Rosso Levanto marble powder/PVA composite is coded as CM3. Structural, spectral, thermal, crystallographic, and mechanical properties of the produced materials were investigated.

2. EXPERIMENTAL

In this study, polyvinyl alcohol (P8136) used for composite material synthesis was obtained from Merck Firm. Its molecular weight is 30,000-70,000 g/mol and its hydrolysis degree is 87-90%. For fabrication of the PVA solution, 8 g of PVA powder was mixed with 92 ml of deionized water at 90 °C for 5 hours. The pH value of the mixture was adjusted to 4 with hydrochloric acid solution (HCl) [14]. After the addition of glutaraldehyde, 5 g of Karaman Beige marble powder was added to the mixture and stirred until a homogeneous mixture was formed. Finally, the mixture was poured into a petri dish and dried at room temperature. After these processes, CM1 composite (filler/matrix; 1/20 by mass) synthesis was completed. The same process was done for CM2 and CM3 composites. The fillers, whose images are given in Figure **1**, were added to the PVA matrix after they were sieved by using an ordinary kitchen sieve to make the powder particles smaller.

The composite materials with different additives in the same proportions were characterized by several tests. Among these, the SEM images of the samples taken by a Zeiss brand EVO MA10 model Scanning Electron Microscope (SEM). The images were taken at 100X and 250X magnifications. By using a Shimadzu DSC-60A model DSC device, the DSC measurements for each composite sample were taken from room temperature to 500 °C at a heating rate of 10 °C/min under 100 ml/min of constant inert argon gas flow. By using a Shimadzu DTG-60AH model DTA-TG instrument the TGA results were obtained by heating the samples from 25 °C to 500 °C at a heating rate of 10 °C/min under the same inert gas flow. The FT-IR tests were taken by using a Thermo Scientific ID4 ATR instrument at room conditions and in the range of 550-4000 cm. The XRD tests were performed in room conditions, at 1.54 Å wavelength, 40 kV voltage and, 40 mA current by using a Bruker brand D8 Advance model XRD instrument in the range of 5-40° scan angle, 0.02° scan step length and, each step of 0.02 seconds. The tensile tests were performed at room temperature under the test conditions specified in DIN EN ISO 527-1 test standard and by using a Zwick brand instrument and all of the different composite samples were used in equal dimensions for these stress-strain tests. In these tensile tests, the pre-load value was 0.1 Mpa, the speed of tensile modulus was 10mm/min, the test speed was 100 mm/min and the grip to grip at the start position was 45 mm.

3. RESULTS AND DISCUSSIONS

In this study, microstructure analyzes were performed with the Zeiss brand EVO MA10 model Scanning Electron Microscope (SEM). The images were taken at 100X and 250X magnifications of produced composite materials with different additives in the same proportions are given in Figure **2**. In all three

Figure 1: Images of fillers before sieving.

images, irregular, sharp corners and partially spherical grains were detected in the microstructure of the composites. Compared to the materials CM1 and CM2 shown in Figure **2a** and Figure **2b** respectively, the best homogeneous distribution was seen in the material CM3 given in Figure **2c**. This result demonstrates that the interaction between the additive material (Rosso Levanto marble powder) and the PVA matrix in this sample is better than the others. Among these SEM images, as seen in Figure **2a** and **3c**, both of the marble dust additions in CM1 and CM3 are seen like micro-sized particles covered by or engulfed in the transparent PVA matrix like a limpid glue. Therefore these micro-sized marble grains, resembling bricks in a mortar, are expected to enhance the mechanical strength (and flexibility) which is to be shown in the tensile test results ahead. In Figure **2b**, the additive fly ash and PVA seems to form a different structure than the ones with marble. This is mostly due to the higher oxygen content in the fly ash which interacted with the carbon (this is to be shown in the FTIR results section ahead) and hydrogen atoms of PVA to form different amorphous forms (depending on the spatial distrubition and effects of metal and other elements) and this must also change the mechanical features to some degree and this is to be shown in the mechanical results, too [15].

Spectroscopic methods are applied in a wide range such as qualitative and quantitative analysis of organic substances, elucidation of their structures, finding stereochemical properties, and purity control [16,17]. FT-IR is a fast, reliable, precise, and inexpensive method used to characterize the chemical composition of materials [18,19].

FT-IR spectroscopy was used for the structural analysis of obtained composites. An interaction occurs between the compounds of the composites. This interaction changes the vibration modes of atoms or molecules in the materials. As a result of this process, the physical and chemical properties of the composite materials differ from each other. Thus, the infrared spectra of the materials varied.

When the FT-IR spectra given in Figure **3** of the samples are examined, the characteristic bands of the PVA polymer can be seen at 3278, 1733, 1643, and 1080 cm^{-1} [14,20]. The peaks observed between 3245-3305 cm^{-1} for CM1, CM2, and CM3 composites represent the –OH stretching that belongs to absorbed water. This peak appears sharper and more violent in composite materials prepared with fillers other than fly ash. Therefore, it can be said that marble powders (Karaman Beige marble powder and Rosso Levanto marble powder) are more compatible with the PVA structure [21]. The stretching vibration of the C=O bond in the carbonyl group was observed at 1733 cm^{-1} and 1730 cm^{-1} in the FT-IR spectra of PVA and CM2 materials, respectively [22]. For CM1 and CM3 composites, this peak occurred at 1789 cm^{-1} and 1796 cm^{-1} wavenumbers, respectively, with very low intensity. The fact that this stretching peak seen in composite materials is less severe than the peak formed in PVA indicates that the hydrogen bond between C=O and –OH is not sufficiently occurred. The stretching vibration of the C=C bond was observed at 1643, 1644, 1652, and 1643 cm^{-1} for PVA, CM1, CM2, and CM3 materials, respectively [23]. Especially for CM1 and CM3 materials, this peak is stronger and formed at almost the same wavenumber as the peak observed in the PVA structure. This result means that the added fillers in these composite materials do not disrupt and also improve the PVA structure [24]. In addition, C–O stretching vibration belonging to the alkoxy group was observed at 1080, 1084, 1080, and 1079 cm^{-1} for PVA, CM1, CM2, and CM3 materials, respectively [25,26]. It is observed that this peak intensity is higher in CM1 and CM3 materials, so it can be mentioned that the fillers compatible with the matrix.

Thermal characterization techniques are used to determine physical and chemical changes such as phase transitions, glass transition temperature (T_g), and melting temperature (T_m). The glass transition temperature (T_g) is an important property for all polymeric composites because it can significantly alter the mechanical behavior of the material. In DSC analysis, the increase in instantaneous heat capacity in the heat exchange curve creates the glass transition temperature (T_g). The glass transition temperature is a quadratic transition and there is no enthalpy associated with the transition. For DSC analysis, a temperature range of 0 - 250 °C was used at a heating rate of 10 °C/min. In this work, the endothermic peaks are the downside peaks and bendings on the curves of the DSC or DTA. Here, the negative enthalpy values displayed on each peak data set belong to the endothermic reactions. In some other labels of DSC/DTA instruments, the enthalpy values of endo peaks are given as positive values. The DSC curves given in Figure **4** show the endothermic peaks of the glass transition temperature (T_g) and the melting temperature (T_m). T_g of polymer blends is a typical characteristic that is used in studying the miscibility and interaction

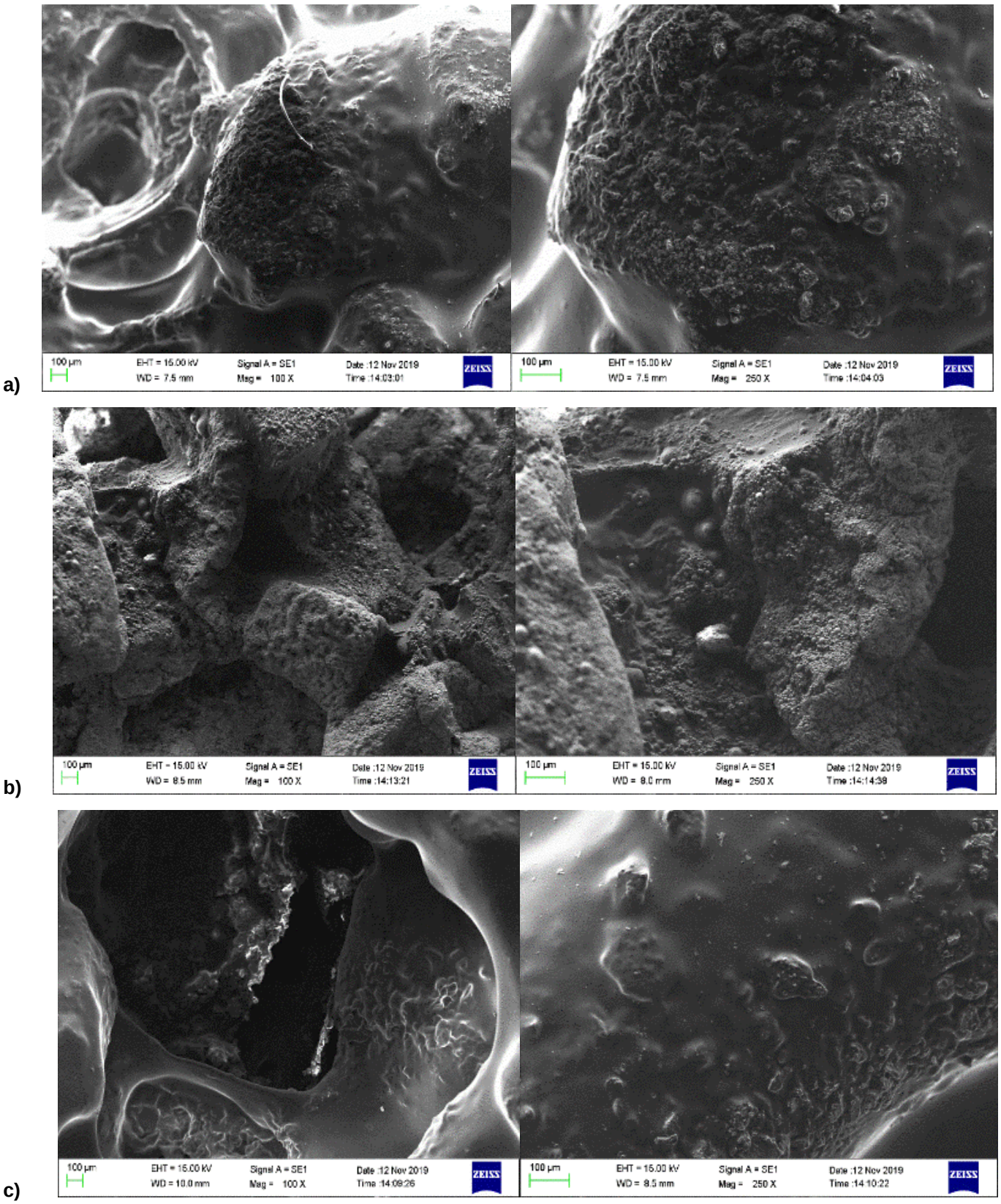

Figure 2: SEM analysis of the samples **a)** CM1, **b)** CM2 and **c)** CM3.

between polymers. T_m is mostly used in investigating the crystallization of polymers [27].

When the DSC curves are examined, three endothermic peaks are similarly seen in all three samples.

The first endothermic peaks give the glass transition temperature of polymeric materials. The second peak shows the crystallization temperatures (T_c) corresponding to the conversion of the crystallizable molecular chains remaining in the structure into crystallized regions due to the temperature during the DSC scan. The final endothermic peak gives the melting temperature associated with the melting of the crystallized regions during the DSC scan [28]. A single peak corresponding to the melting temperature was obtained in all samples. The glass transition temperatures, cold crystallization temperatures, and melting temperatures of the polymeric composites determined from the DSC curves shown in Figure **4** are given in Table **1**.

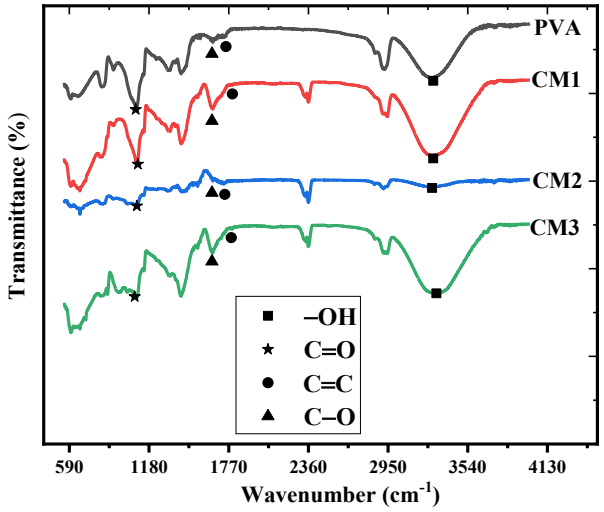

Figure 3: FT-IR spectra of the produced materials.

Table 1: Thermal Properties of Polymeric Composites Dependent on DSC Spectrum

Samples	T_g (°C)	T_c (°C)	T_m (°C)
CM1	76.2	229.9	290.1
CM2	104.6	234.5	267.3
CM3	71.7	221.6	276.1

When the glass transition temperatures of the materials are examined, it is seen that the CM3 sample has the lowest value with 71.7 °C. This result indicates that this material is more flexible than the others [29]. The more flexible the chain, the lower the glass transition temperature [30].

Thermal analysis is used for the examination of polymers, alloys, complexes, salts, etc. thermal properties and for quality control purposes [31]. Thermogravimetry (TG) is used to determine the stoichiometry by examining the change in the mass of the sample against temperature increase. This method is also used to interpret the thermal stability of the sample. Differential Thermal Analysis (DTA) is frequently used to determine the decomposition events and temperature ranges of samples, enthalpy of state change, endothermic-exothermic reactions [32].

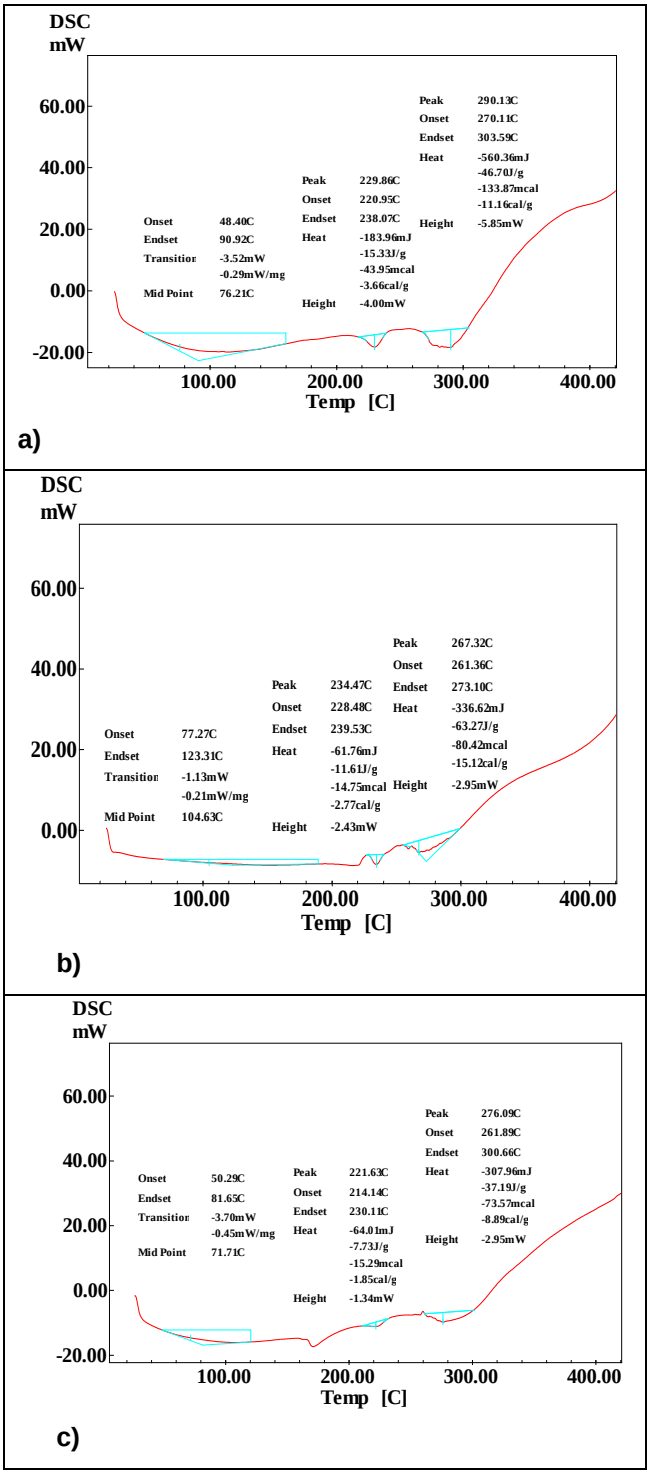

Figure 4: DSC curves of the samples **a)** CM1, **b)** CM2 and **c)** CM3.

Thermograms given in Figure **5** were obtained by heating from 25 °C to 500 °C under argon gas at a heating rate of 10 °C/min. When the TGA thermogram of the CM1 sample given in Figure **5a** is examined, a three-step decomposition curve appears. It is seen that the first mass loss is 13.2% and is caused by the removal of moisture generated by the water molecules physically contained in the polymer, which corresponds to the endothermic downfall on the DTA curve starting from the far left at room temperature to ~150 °C. The second and largest mass loss in the decay curve is 30.7% and is between 271 °C and 296 °C corresponds to the largest endo DTA peak at around 284.5 °C. This region of greatest mass loss in the TGA curve is directly related to the degradation of the PVA structure [33]. In this region, the main and side chains in the PVA structure are separated from each other [34]. The mass loss in the third zone is between 308 °C and 324 °C and is 10.7% corresponding to the right side of the largest DTA peak. Mass loss in the third zone is caused by the breakdown (degradation) of the PVA main chain [33]. The mass remaining as a result of all these degradations is 5.9 mg. The TGA thermogram given in Figure **5b** shows a two-stage decay curve. The first mass loss for the CM2 sample is observed between 265°C - 282°C and 43.8% corresponding to the combination of the first and smaller endo peak and the largest endo peak on DTA led by the degradation of PVA. The second mass loss is 12.9% between 300 °C and 500 °C due to the combustion of residual PVA or the intermediate compounds from degraded PVA. When the TGA thermogram given in Figure **5c** is examined, the first mass loss is caused by the removal of moisture in the structure and it is seen that it is between 57 °C - 152 °C and 7.5%. The second and largest mass loss caused by the degradation of PVA seen in the decay curve is mainly between 267 °C and 306 °C with a value of 34.8%. The third mass loss caused by the combustion of residual PVA for the CM3 sample is between 315 °C-429 °C and 13.1%. According to the TGA curve, the mass loss amount in the CM3 sample is lower than in other samples. Therefore, this tendency of the CM3 material is positive at the thermal stability issue.

X-ray diffractometry (XRD) is a device used to obtain information about the crystalline structure of semi-crystalline polymers in the range of 0.1 to 0.5 nm between atoms [35]. With the X-ray diffraction method, detailed information can be obtained about the chemical composition and crystal structure of natural or produced materials such as rocks, crystalline, thin-film, and polymer. XRD method has advantages such as not destroying the material during analysis, being able to analyze amorphous materials, and even small amounts

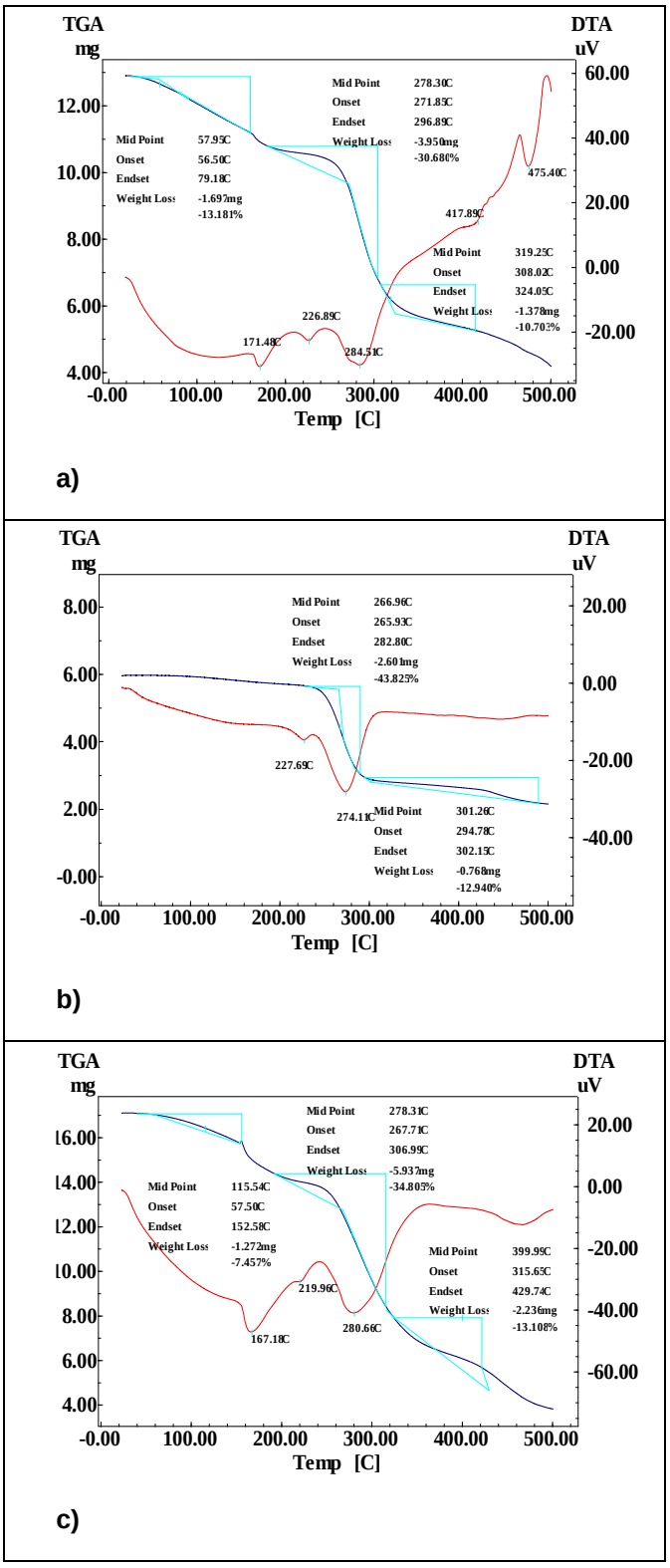

Figure 5: TGA-DTA curves of the samples **a)** CM1, **b)** CM2 and **c)** CM3.

of samples [34]. Tests were performed at 1.54 Å wavelength, 40 kV voltage, and 40 mA current by Bruker brand D8 Advance model XRD. Spectra given in Figure **6** were obtained in the range of 5-40° scan angle, 0.02° scan step length, and each step 0.02 seconds. When Figure **6** is examined, a sharp peak in the range of 0-30° is not seen. This result may be due to the small size of the crystalline portions of the materials, the density of the amorphous region, or the distribution of the crystalline region within the structure. The maximum peaks of the materials were seen at 30-33°. When the XRD curve of the CM3 sample is examined, it is seen that the characteristic peak density is more pronounced than the others. This means that cross-linking induced by the addition of Rosso Levanto marble powder increases the crystallinity of the composite material to some extent. In the CM1 sample, some microcrystals remain in the polymer chain, probably due to the high crystallinity of PVA. Therefore, the cross-links partly reduce the degree of freedom in the polymer chains and limit the formation of crystalline regions.

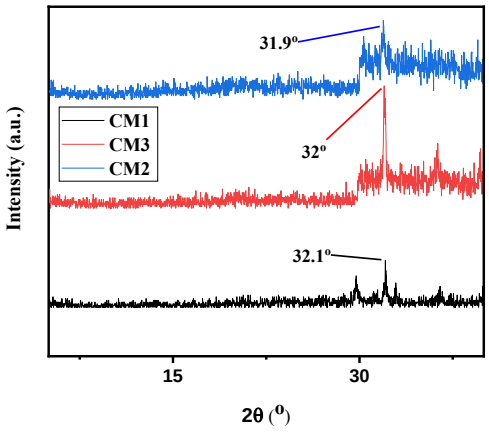

Figure 6: XRD curves of composite materials.

To determine the elastic and plastic behavior of the materials under static load, a stress-strain test was performed. The tests were carried out under the test conditions specified in ISO 527-1 standard and on Zwick brand device. All materials were used in equal dimensions for the stress-strain test. The results are given in Table **2**.

Table 2: Results of the Stress-Strain Test.

Samples	E_t (MPa)	σ_m (MPa)	ε_m (%)	σ_b (MPa)	ε_b (%)
CM1	17.2	1.0	5.8	0.8	6.3
CM2	3.0	2.8	10.0	2.8	10.0
CM3	53.1	4.0	5.8	0.8	13.0

Here E_t (modulus), the slope of the stress/strain curve $\sigma(\varepsilon)$ in the strain interval between ε_1=0.05% and ε_2=0.25%. ε_m (strain at strength), strain at which the strength. ε_b (strain at break), strain at the last recorded data point before the stress is reduced to less than or equal to 10 % of the strength if the break occurs before yielding. σ_m (strength), stress at the first local maximum observed during a tensile test. σ_b (stress at break), stress at which the specimen breaks [36]. When the tensile test results given in Table **2** are examined, it is seen that the tensile strength of the CM3 material is 4.0 MPa and the strain value is 5.8%. The modulus of elasticity is defined as bond strength containing two atoms. This value refers to the strength of the material. According to tensile test results, the material with the highest strength value is CM3. The value of elasticity is a characteristic property that belongs to the material. As the elasticity value increases, it can be said that the bond strength between atoms increases. And also, it can be said that strength and yield stress are increased.

4. CONCLUSIONS

In this study, when the SEM images of polymeric composite materials produced in a ratio of 1:20 by mass are compared, it is seen that the best homogeneous distribution is CM3. This result shows that the interaction between the additive (Rosso Levanto marble powder) and the PVA matrix in this example is better than CM1 and CM1 composite materials.

The ratios of the atoms and compounds that make up the used fillers are different from each other. This difference causes the physical and chemical properties of the composite materials to differ from each other. Therefore, the intensity of the obtained characteristic peaks as a result of FT-IR analysis varies for each material. FT-IR spectra clearly show the difference between these materials.

When the DSC analysis results are examined, it is seen that the material with the lowest glass transition temperature and the lowest crystallization temperatures is CM3. If the chain in the material structure is flexible, the glass transition temperature is also low. Therefore, it can be concluded that the most flexible material with the lowest glass transition temperature value is CM3 among these materials.

Thermogravimetric analysis of CM1 and CM3 samples show three distinct steps of weight loss, the first step corresponds to the removal of water, the

second step is due to thermal degradation of intermolecular hydrogen bonding and the third step leads to the decomposition of the main backbone chain. The TGA thermogram of the CM2 sample shows a two-step decomposition curve. As a result, it can be said that all three materials have approximately the same mass loss between the same temperature values.

According to XRD analysis results, maximum peaks of all three materials were observed between 30-33°. The characteristic peak density of the CM3 sample is more pronounced than the others. This means that crosslinking induced by the addition of Rosso Levanto marble powder increases the crystallinity of the composite material to some extent. This data is consistent with other analysis results.

When tensile test results are examined, it is seen that CM3 material is the most flexible material with a tensile strength value of 4.0 MPa and a strain value of 5.8%. The elasticity modulus of this material is higher than other materials with a value of 53.1 MPa. This result indicates that the strength property of CM3 material has the highest value. When all these analysis results are taken into consideration, it can be concluded that Rosso Levanto marble powder is the most compatible with PVA in different fill materials used in the same proportions. The homogeneity of the structure of this material, which has the highest elasticity and strength, makes this material more preferable according to need.

REFERENCES

[1] Bucher, Kurt, and Rodney Grapes. Petrogenesis of Metamorphic Rocks. (Springer, Berlin, Heidelberg, (**2011**), pp. 225-255. https://doi.org/10.1007/978-3-540-74169-5_6

[2] Alyamaç, Kürşat Esat, and Ragip Ince. Constr. Build. Mater. 23.3: 1201-1210 (**2009**). https://doi.org/10.1016/j.conbuildmat.2008.08.012

[3] Hubbard, H. A., and Ericksen, G. E., in Brobst D. A., and Pratt, W. P., eds., United States mineral resources: U.S. Geology. (**1973**), v. 38, nos. 3 and 4, pp. 303-364.

[4] Gao, N. F., Kume, S., & Watari, K., Mater. Sci. Eng. A. 399(1-2), 216-221 **(2005)**. https://doi.org/10.1016/j.msea.2005.04.008

[5] Ünal, M. T., & Şimşek, O., Politeknik Dergisi. **(2020)**.

[6] Rozenstrauha, I., Bajare, D., Cimdins, R., Berzina, L., Bossert, J., & Boccaccini, A. R., Ceram. Int, 32(2), 115-119 (**2006**). https://doi.org/10.1016/j.ceramint.2005.01.006

[7] Siotto, G., Careddu, N., Curreli, L., Marras, G., & Orru, G., in Dımensıon Stones-Xxı Century Challenges, 2nd Internatıonal Congress On Dımensıon Stones. Pacini Editore. (**2008**), pp 387-390.

[8] Terzi, S. Karasahin, M. Technical Journal, Volume: 193, 2903-2922 (**2003**).

[9] Hristova, J., Valeva, V., & Ivanova, J. Compos. Sci. Technol, 62(7-8), 1097-1103 (**2002**). https://doi.org/10.1016/S0266-3538(02)00055-6

[10] Khrıstova, Yu; Anıskevıch, K., Mechanic Composite Material, 30: 590-599 (**1994**).

[11] García-Ten, J., *et al*., in CFI Ceramic Forum International. Goeller Verlag GmbH, (**2003**).

[12] Ali, M. M., *et al*., Cem. Concr. Res. 30(6), 977-980 (**2000**). https://doi.org/10.1016/S0008-8846(00)00258-1

[13] Ohama, Y., Adv. Cem. Based Mater., 5(2), 31-40 (**1997**). https://doi.org/10.1016/S1065-7355(96)00005-3

[14] Ünlü, N., & Canbay, C. A., JMED 3(1), 8-13 (**2020**). https://doi.org/10.1007/s13538-020-00823-1

[15] Hayat, M. Arif, ed. Principles and techniques of scanning elektron microscopy: biological applications (**1978**).

[16] Erdik, E., Organik kimyada spektroskopik yöntemler. Gazi Büro Kitabevi. (**1993**).

[17] Dogan, A., Siyakus, G., & Severcan, F., Food Chem., 100(3), 1106-1114 (**2007**). https://doi.org/10.1016/j.foodchem.2005.11.017

[18] Bhat, R., Int. J. Food Prop. 16(8), 1819-1829 (**2013**). https://doi.org/10.1080/10942912.2011.609629

[19] Ergin, Ç., İlkit, M., Gök, Y., Özel, M. Z., Çon, A. H., Kabay, N., & Döğen, A., J. Microbiol. Methods, 93(3), 218-223 (**2013**). https://doi.org/10.1016/j.mimet.2013.03.011

[20] Ding, W., Wei, S., Zhu, J., Chen, X., Rutman, D., & Guo, Z., Macromol Mater Eng. 295(10), 958-965 (**2010**). https://doi.org/10.1002/mame.201000188

[21] Luo, X., Wang, C., Luo, S., Dong, R., Tu, X., & Zeng, G., Chem. Eng. J. 187, 45-52 (**2012**). https://doi.org/10.1016/j.cej.2012.01.073

[22] Li, N., Zheng, M., Chang, X., Ji, G., Lu, H., Xue, L., & Cao, J., J. Solid State Chem, 184(4), 953-958 (**2011**). https://doi.org/10.1016/j.jssc.2011.01.014

[23] Tang, G., Jiang, Z. G., Li, X., Zhang, H. B., Dasari, A., & Yu, Z. Z., Carbon, 77, 592-599 (**2014**). https://doi.org/10.1016/j.carbon.2014.05.063

[24] Andrijanto, E., Shoelarta, S., Subiyanto, G., & Rifki, S., in AIP Conference Proceedings, AIP Publishing LLC. (**2016**), Vol. 1725, No. 1, p. 020003.

[25] Chhatri, A., Bajpai, J., Bajpai, A. K., Sandhu, S. S., Jain, N., & Biswas, J., Carbohydr. Polym. 83(2), 876-882 **(2011)**. https://doi.org/10.1016/j.carbpol.2010.08.077

[26] Kumar, G. H., Rao, J. L., Gopal, N. O., Narasimhulu, K. V., Chakradhar, R. P. S., & Rajulu, A. V., Polymer, 45(16), 5407-5415 (**2004**). https://doi.org/10.1016/j.polymer.2004.05.068

[27] S. J. Liu, Int. Polymer Proc. XIII, Hanser Publishers, (Munich, **1998)**, pp. 88–90.

[28] Söylemez, Ertan., MS thesis. Hitit Üniversitesi Fen Bilimleri Enstitüsü, 2016.

[29] Tiyek, İ., Donmez, U., Yildirim, B., Alma, M.H., Ersoy, M.S., Karatas, S., Yazici, M., SAU Science Journal 20. Volume, 2. Issue, p. 349-357 (**2016**). https://doi.org/10.16984/saufenbilder.29009

[30] Lee, L. J., Zeng, C., Cao, X., Han, X., Shen, J., & Xu, G., Compos Sci Technol, 65(15-16), 2344-2363 (**2005**). https://doi.org/10.1016/j.compscitech.2005.06.016

[31] Flynn, J. H., Schwenker, R. F., & Garn, P. D., Academic Press, (New York, **1969**).

[32] Dee, P. P., N. Roy Choudhury, and N. K. Dutta., ISmithers Rapra Pub., (**2010**).

[33] Anbarasan, R., Pandiarajaguru, R., Prabhu, R., Dhanalakshmi, V., Jayalakshmi, A., Dhanalakshmi, B., Nisha, S.U., Gandhi, S., Jayalakshmi, T., J. Appl. Polym. Sci. 117, 2059–2068 (**2010**). https://doi.org/10.1002/app.32033

[34] Shao, C., Kim, H. Y., Gong, J., Ding, B., Lee, D. R., & Park, S., J. Mater. Lett 57(9-10), 1579-1584 (**2003**). https://doi.org/10.1016/S0167-577X(02)01036-4

[35] Cullity, B. D., Reading, (USA, **1978**), pp. 32-106. https://doi.org/10.1515/hfsg.1978.32.3.106

[36] ASM Handbook, "Mechanical Testing" Tenth Ed., ASM, (Ohio, **1998)**.

Received on 05-11-2020 Accepted on 06-12-2020 Published on 29-12-2020

DOI: https://doi.org/10.31875/2410-4701.2020.07.07